ELSEVIER

Contents lists available at ScienceDirect

Journal of Environmental Chemical Engineering

journal homepage: www.elsevier.com/locate/jece



Hydrothermal oxidation of MEA-triazine spent and unspent H₂S scavengers in continuous-flow reactor

Alessandro Perrucci ^a, Lars Michael Skjolding ^b, Sarah Fredung Hückelkamp ^c, Sofie Askjær Hass ^c, Maria Nymann Christensen ^c, Jens Muff ^a, Marco Maschietti ^{a,*}

- a Department of Chemistry and Bioscience, Section of Chemical and BioEngineering, Aalborg University, Niels Bohrs Vej 8A, Esbjerg 6700, Denmark
- ^b Department of Environmental and Resource Engineering, Technical University of Denmark, 2800 Kgs, Lyngby, Denmark

ARTICLE INFO

Keywords:
Spent scavengers
Hydrogen sulfide
MEA-triazine
Dithiazine
H₂S scavenging
Hydrothermal oxidation
Wet air oxidation

ABSTRACT

The removal of hydrogen sulfide by injecting MEA-triazine in produced gas generates a wastewater (spent and unspent scavengers: SUS) that in offshore practice is often discharged untreated into the sea, thereby contributing largely to the environmental footprint of oil and gas fields. In this work, the feasibility of Hydrothermal Oxidation (HTO) of SUS in continuous-flow mode of operation (SUS flow rate 0.48–0.65 L/h) was investigated in a reactor operated at 24 MPa and 325–350 °C, for residence times of 9–23 min. Four SUS samples were used: two from a North Sea installation and two related samples obtained by nanofiltration. The study proved the feasibility of HTO for feeds with chemical oxygen demand (COD) up to 168 g/L, under autothermal conditions. Higher COD values proved problematic for temperature control under near-critical water conditions. The COD and total organic carbon (TOC) of the liquid effluent were reduced by 91 %-99 % and 86 %-100 %, respectively, while the ecotoxicity was reduced by more than 99 % and 94 %-98 % towards marine bacteria and algae, respectively. The effect of the feed COD on the buffer capacity of the reacting system is discussed, highlighting its importance in preventing pH drops within the HTO reactor. Increasing the pH of the feed proved necessary for the SUS permeate feeds, and positive for reducing carbon monoxide in the gas effluent for all feed types. The main reaction products in the liquid effluent were ammonium, sulfate, and acetic acid. An extensive analytical characterization of both the liquid and gas effluent is provided.

1. Introduction

Hydrogen sulfide (H_2S) occurs naturally and is encountered in oil and gas reservoirs. H_2S is an extremely hazardous gas with pungent rotten-egg odor. It is colorless, flammable, highly toxic, corrosive (in the presence of water), and soluble in both water, hydrocarbons, and other organic solvents [1–3]. Natural gas pipeline transportation systems typically require the H_2S content to be below about 4 ppmv [4].

In topside offshore oil and gas installations, the removal of H_2S from the produced gas is typically accomplished by direct injection of liquid H_2S scavengers into the wet gas stream. These scavengers are chemical agents which react fast with H_2S , thereby converting it into markedly less hazardous and corrosive compounds [5]. Downstream of the injection point, the gas and the liquid phase are separated. The scavenging reaction products, as well as any unreacted scavenger, are collected in the liquid phase, while the gas is conveyed to dehydration, compression,

and piping for export [6]. The most widely used H_2S scavenger is 1,3, 5-tris-(2-hydroxyethyl)-hexahydro-s-triazine (HET), also known as MEA-triazine, which is commercialized as an aqueous solution typically in the range of 30–60 % by mass. Its success is due to low cost, simple synthesis, high pH of the aqueous solution enhancing the absorption of H_2S , and high reaction rates with H_2S in the aqueous phase [5–10]. The recognized reaction scheme between H_2S and HET consists of two reactions in series (Fig. 1). Initially, 3,5-bis-(2-hydroxyethyl)hexahydro-1, 3,5-thiadiazine (thiadiazine, TDZ) and monoethanolamine (MEA) are formed. Subsequently, 5-(2-hydroxyethyl)-hexahydro-1,3,5-dithiazine (dithiazine, DTZ) and another MEA molecule are produced in the second reaction [7–10].

In topside offshore gas treatment, a large excess of MEA-triazine is used to ensure fast reaction rates, therefore preventing H_2S to exceed the maximum allowable limits in the downstream pipeline transportation, and to prevent fouling of pipes and equipment. Consequently, the

E-mail address: marco@bio.aau.dk (M. Maschietti).

^c Aquarden Technologies ApS, Industrivej 17, Skævinge 3320, Denmark

^{*} Corresponding author.

scavenging process generates a wastewater containing the reaction products MEA, TDZ, and DTZ, as well as large amount of unreacted HET. This wastewater is indicated in the following as Spent and Unspent Scavenger (SUS). Low concentration of pollutants such as formaldehyde, trithiolanes and tetrathiepanes may also be found in the SUS [5,6]. In addition, solid precipitates of amorphous polymeric dithiazine (apDTZ) may be formed at high degree spent [11]. The properties of six SUS samples collected in offshore installations in the North Sea were reported in a previous work, where the samples showed high levels of Total Organic Carbon (TOC) (36-123 g/L) and Chemical Oxygen Demand (COD) (120 - 320 g/L), and a pH in the range of 8.9 - 9.6 [12]. Because of the fouling and scaling potential caused by the high pH and the high concentration of organics, this wastewater is often problematic to inject in disposal wells in offshore practice. In addition, no on-site offshore methods for treating the SUS have proved feasible so far. Consequently, in offshore operations the SUS is often discharged into the sea without any treatment. Despite the small volume (typically less than 0.1 % of the total offshore produced water volume), the SUS is a relevant contributor to the Environmental Impact Factor (EIF) of oil and gas fields. For example, Stipanicev et al. [13] reported that the discharge of the overdosed HET contained in the SUS contributed to 20 % of the EIF of two North Sea fields. Montesantos et al. [14] reported ecotoxicity data on SUS, showing that even after diluting the SUS sample approximately 4200 times and 23,000 times, 50 % inhibition for bacterial luminescence (Aliivibrio fischeri) and for algal growth (Skeletonema pseudocostatum), respectively, was still observed. This is significantly higher than the dilution factors of 9.1 for bacteria and 14 for algae for offshore produced water, required to achieve the same level of inhibition [14]. The small volume of SUS and the large contribution to the EIF of oil and gas fields suggest the feasibility and the potential environmental benefit of a low-volume on-site treatment unit of the SUS before discharge.

A suitable method for significantly reducing the organic pollutants in medium-high concentrated industrial wastewaters (COD 20 – 200 g/L) is Hydrothermal Oxidation (HTO) at subcritical conditions, also known as Wet Oxidation [15]. It removes organic compounds in the aqueous phase using an oxidant (e.g., air or pure oxygen), at high pressure and high temperature (typically 2 – 20 MPa and 175 – 320 °C), by oxidizing them to carbon dioxide and water [15,16], while nitrogen- and sulfur-containing compounds are converted to ammonium, nitrate, nitrogen gas, sulfuric acid or sulfate [16]. HTO application is more common under subcritical conditions, as supercritical conditions pose several challenges for industrial purposes, such as scale formation, corrosion, and instability [17,18]. An example of HTO application on wastewaters containing organic nitrogen and organic sulfur is the

treatment of spent caustic solutions generated by, e.g., ethylene production plants [19,20]. In HTO, the heat generated by the oxidation reaction (typically around 100 kcal/mol of reacted O₂) maintains the operating temperature of the reactor [21]. According to Debellefontaine et al. [17], the process becomes autothermal at COD levels above just 12–15 g/L.

Montesantos et al. [6,14] demonstrated the effectiveness of HTO on offshore SUS samples in batch-mode at laboratory scale, where the effect of temperature, oxygen supply and reaction time was studied. By operating on a diluted SUS (feed COD of approximately 30 g/L), a COD reduction above 90 % was obtained with a reaction time of 20 min or longer. Additionally, the toxicity of the feed towards marine bacteria was reduced more than 90 % at all conditions tested, while the reduction ranged from 48 % to 86 % towards algae, depending on the specific process conditions [14]. Furthermore, a second-order rate equation with respect to COD was determined to effectively describe the rate of COD consumption, with the rate constant at 350 °C being 66 times higher compared to that at 200 °C. The analysis of the liquid reaction products indicated the presence of some intermediate oxidation products such as pyrazines, pyridines, and short-chain carboxylic acids (C1-C4). Organic nitrogen mostly ended up as ammonium, with only small amounts of nitrate detected at 200 °C, and organic sulfur primarily ended up as sulfate [6]. However, neither tests at different feed pH nor different feed COD were conducted. In addition, the gas effluent was not analyzed in these works. The feed pH is expected to play an important role in the reaction pathways, kinetics, as well as on corrosion and reactor material stability [22]. Moreover, to validate the technology and its operation in continuous-flow for large-scale applications, different levels of feed COD must be tested. Furthermore, the gas analysis is crucial to ensure compliance with environmental and safety regulations.

Previous works demonstrated the possibility to recover unreacted MEA-triazine from the SUS by means of nanofiltration (NF), which is a technology that could lead to recycling unspent MEA-triazine in the direct injection process. The application of the membrane separation generates a permeate characterized by a higher sulfur-to-nitrogen ratio compared to the unseparated SUS [23–25], whereby the permeate represents a modified type of SUS. The availability of different samples of SUS from offshore installations, along with the production of SUS-derived samples obtained through membrane separation, allows investigating the HTO process on a variety of SUS-type feeds and, therefore, testing the flexibility of the process with respect to feed variations.

The aim of this work is to validate the HTO technology on SUS in continuous-flow mode operation. An experimental campaign was

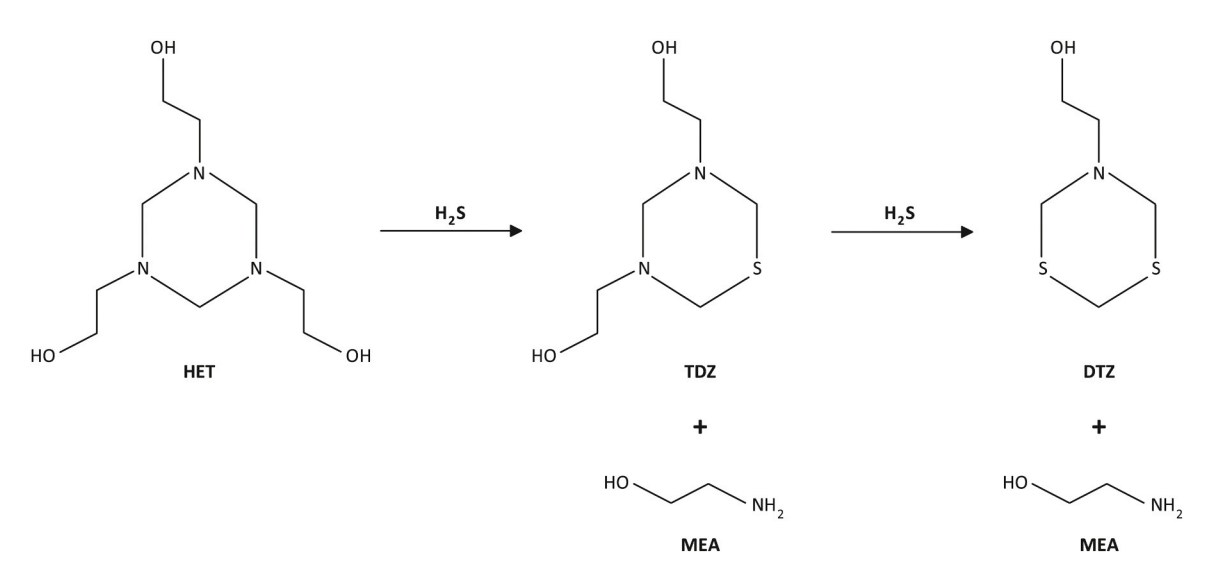


Fig. 1. Simplified H₂S scavenging reaction scheme with MEA-triazine.

conducted using a vertical high-pressure high-temperature reactor operating at around 325 - 350 $^{\circ}\text{C}$ and 24 MPa and using oxygenenriched air as oxidant. To evaluate the flexibility of the HTO process, four different feeds were used. The effects of the feed pH and COD on the operability of the process were studied. In addition, the composition of the gas effluent was analyzed.

2. Materials and methods

2.1. Materials

Two SUS samples were used in this work (SUS A and SUS B), which were collected in a North Sea offshore platform in August 2020 and June 2023, respectively, and stored at 4 $^{\circ}\text{C}$ since the delivery time. The SUS samples result from scavenging the produced gas by direct injection of MEA-triazine, followed by phase separation in two separators. In the first separator, two liquid phases, which consist of gas condensates and the SUS wastewater are separated from the gas, while in the second, the SUS is separated from the gas condensates. The sample SUS A was homogeneous, while suspended solids with a tendency of precipitating over time were visible in the sample SUS B. Prior to using SUS B in the experimental campaign, the sample was subjected to microfiltration through a Matest 50 μ m metal wire cloth sieve. SUS A was clear orange/light brownish, whereas SUS B after microfiltration was light yellow, both with pungent sulfur and fishy odor.

In addition to SUS A and SUS B, HTO experimental runs were also conducted on their corresponding permeates, SUS A-P and SUS B-P, which were obtained by separating SUS A and SUS B using nanofiltration. The separation was carried out by preliminary microfiltration on a sheet polysulfone membrane with a pore size of 0.2 µm (Alfa Laval MFG2) followed by nanofiltration on a flat sheet polyamide membrane (FilmTecTM NF270, Dupont). The feed was split into a permeate and a retentate, with a permeate/feed volumetric ratio of 0.50. Since MEA-triazine is preferentially retained by the nanofiltration membrane, the permeate is characterized by a lower HET/DTZ ratio and a lower nitrogen/sulfur ratio. Since these permeate samples are enriched in the spent compounds they are indicated as "spent scavengers" henceforth in this paper. Further details on the equipment and procedure of the membrane separation can be found elsewhere [24]. The four different samples are shown in Fig. 2.

For analysis with high-performance liquid chromatography (HPLC), the following carboxylic acids were used as calibration standards: oxalic (≥ 99 %), succinic (≥ 99.5 %) and maleic (≥ 99 %) acid from Merck, formic (≥ 95 %) and glycolic (≥ 99 %) acid from Sigma-Aldrich, and acetic acid (≥ 99.7 %) from VWR. Furthermore, sulfuric acid (98%) was used as eluent. Sodium carbonate (≥ 99.9 %) and sodium bicarbonate (≥ 99.9 %) from VWR were used to prepare standard solutions for total inorganic carbon (TIC) measurements and as eluents for ion



Fig. 2. Left: spent and unspent scavengers SUS A and SUS B (after removal of the suspended solid by nanofiltration). Right: spent scavengers SUS A-P and SUS B-P.

chromatography (IC). Ion chromatography multi-element standard from Reagecon was used to prepare standard solutions for IC calibration. Potassium hydrogen phthalate (≥99.9 %) from VWR was used to prepare standard solutions for total carbon (TC) measurements. Pyrazine (≥99 %) from Sigma-Aldrich and pyridine (>99 %) from Acros were used as analytical standards for gas chromatography - mass spectrometry (GC-MS) to make calibration curves. Dichloromethane (DCM, ≥98 %) and 2-bromopyridine (>99 %) from Sigma-Aldrich were used as extraction solvent and as internal standard, respectively, for GC-MS. Spectroquant cell test kits from Merck were used to quantify total nitrogen (1.14763) and ammonium-N (1.14558, 1.14544). The chemical oxygen demand (COD) was quantified with the Merck spectroquant cell (1.01797, 1.14555) and with Hach Lange cuvette tests (LCK 014, 914). The density and pH of the SUS, the spent scavengers and the HTO liquid effluents were measured on an AntonParr DMA 35 EX and Metrohm 913 pH meter, respectively.

2.2. Hydrothermal oxidation experiments

The HTO setup is located within the facilities of Aquarden Technologies. The schematic, provided by Aquarden Technologies, is shown in Fig. 3. The core of the setup is the HTO continuous-flow reactor, which is a high-pressure high-temperature column. An HTO experiment started by pumping demineralized water into the bottom of the reactor using a high-pressure pump, while simultaneously injecting compressed oxygen-enriched air and heating up the system. For safety reasons, the oxygen mole fraction in the compressed air was not allowed to exceed 0.40. However, due to other operations at the Aquarden Technologies facility, the oxygen mole fraction varied throughout the experimental campaign. In the experimental runs of this work the mole fraction of oxygen in the gas feed was in the range 0.22 - 0.38. The HTO reactor is thermally insulated and equipped with three heating elements, which provide heat during the start-up of the system. The heating elements can be operated independently, allowing flexibility in the temperature control in the reactor. The temperature is measured on the reactor outside wall by thermocouples. Depending on the COD load of the SUS feed water, the reactor was either heated to the operationally desired temperature or to 15 °C below before the SUS feed was introduced. With higher COD loads (>120 g/L), the exothermic oxidation reactions raised the reactor wall temperature by approximately 15 °C, hence necessitating the lower start temperature. While flowing upward through the reactor, the reacting mixture is heated by the reaction products, which flow downward and are warmer due to the heat generated by the exothermic oxidation reactions. This is accomplished by an internal heat exchanger, which is designed to distribute the heat generated by the oxidation reactions throughout the reactor. The residence time of the reacting mixture in the reactor was estimated by an approximate procedure assuming ideal co-current flow with negligible phase slip. Under these conditions, the residence time can be estimated from the total volumetric flow rate (gas + liquid), at the reactor conditions of pressure and temperature, and the reactor volume. The calculations of the volumetric flow rates at the reactor conditions were based on the mass flow rate of the SUS and on the volumetric flow rate of gas feed at normal conditions and on the experimental density of water (instead of SUS) and air (instead of oxygen-enriched air) at the pressure and temperature of the reactor. In these experiments, the residence time ranged from 9 to 23 min. The reaction products are filtered, expanded to atmospheric pressure in a back pressure control valve and separated in a gas-liquid separator. The liquid effluent was collected into a tank, and the gas effluent vented to the atmosphere. Pressures and temperatures of the fluid mixtures are measured at both the inlet and the outlet of the reactor. The oxygen concentration in the gas products was measured online. In addition, the pH of the liquid effluent was continuously measured using an online pH-meter (Testo 206).

It took approximately 90 min from the start of the introduction of the SUS wastewater to reach steady state conditions. The system was

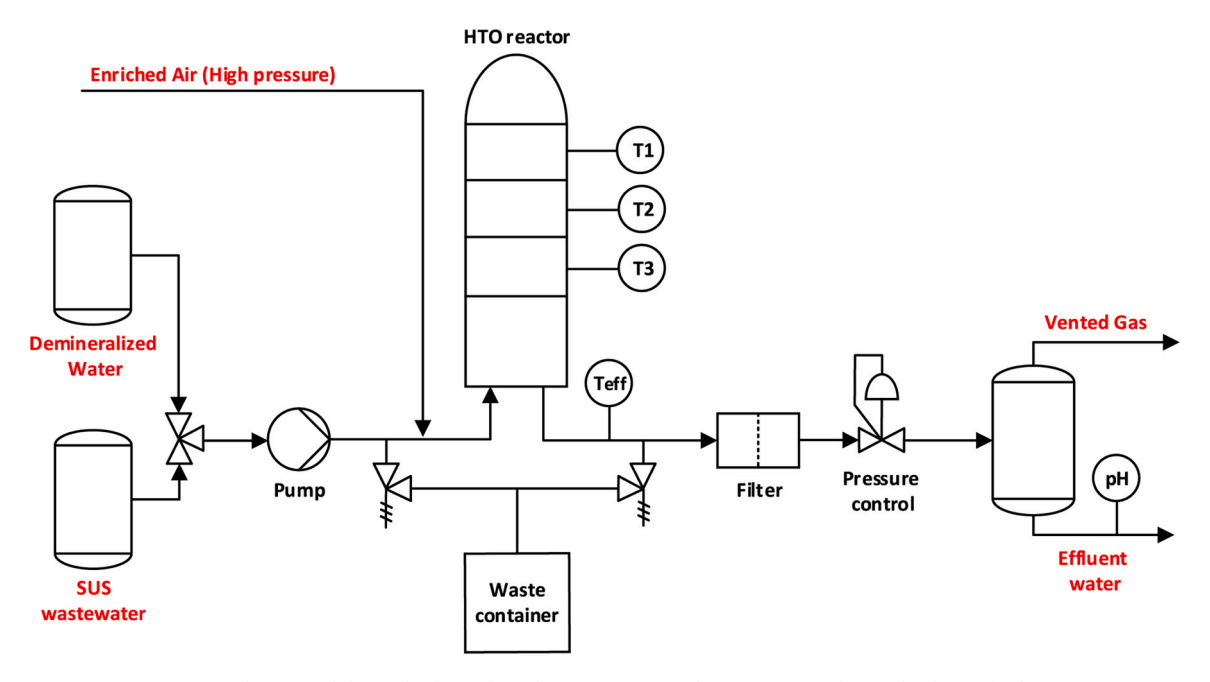


Fig. 3. Schematic of the Hydrothermal Oxidation experimental setup at Aquarden Technologies facility.

considered to be at steady state when the reactor wall temperatures had only small fluctuations (\pm 5 °C) and the average effluent temperature did not show any further increasing trend. An example of the observed trends is shown in Fig. 4. At steady state conditions, no additional heat was applied to the system for all runs, thus showing that the reaction was autothermal for all the feed COD values subjected to investigation, i.e., 27-165 g/L. As T1, T2, and T3 are temperatures measured on the reactor outside wall, internal spatial temperature gradients and larger time fluctuations cannot be excluded for the subcritical fluid, which may not be registered by the wall temperature measurements. Higher feed COD led to higher temperatures of the effluents, as shown in Figure S1 and Table S1 in the Supplementary information.

When steady state conditions were reached, the liquid effluent was sampled for 60–90 min, and its flow rate measured gravimetrically. The gas effluent was also sampled during the steady state period, where two gas samples of 1 L (volume metered at ambient conditions) were collected consecutively in gas sampling bags (SKC, Flex Foil Plus). An online flue gas analyzer (Testo 340) was used to measure sulfur dioxide (SO₂), nitrogen dioxide (NO₂), carbon monoxide (CO) and oxygen (O₂) concentrations in the gas phase.

After approximately 90 min of steady state operation, the shutdown procedure was started by switching the feed to a solution of 0.5–2 wt% sodium hydroxide. The alkaline shutdown solution was used to prevent a possible pH drop leading to the formation of sulfuric and nitric acid, which could cause corrosion of the reactor materials. The sodium hydroxide concentration utilized in the shutdown depended on the COD

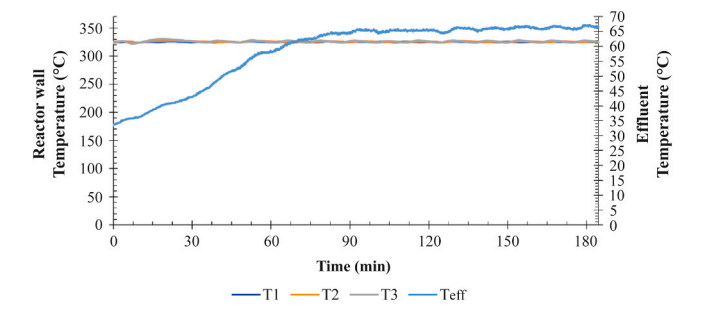


Fig. 4. Reactor outside wall temperature (left axis) and effluent temperature (right axis) profiles.

load of SUS feed. The shutdown procedure took approximately 2 h.

2.3. Analytical procedures

The Merck spectroquant cell test kits used for COD measurements covered ranges of 0.5-10 g/L and 5-90 g/L, while those from Hach Lange were for COD of 1–10 g/L and 5–60 g/L. The COD of the SUS was measured in two dilution ranges (with Merck kits), while the feed COD and HTO products were measured in the other ranges (with Hach Lange kits). On each dilution a triplicate measurement was carried out, with a relative standard deviation (RSD) always below 3 % of the average value. TIC and TC, with TOC calculated by their difference, were measured by using thermocatalytic high-temperature digestion, as described by Montesantos et al. [6]. Total sulfur (TS) was measured at Eurofins (Denmark) via ICP-OES following the standards SM 3120, DS 259:2003, with a declared percentage uncertainty of 20 %. The analytical procedures for quantitating total nitrogen (TN) and ammonium-N were applied according to the methods reported by Montesantos at al. [6]. Short-chain carboxylic acids (i.e., oxalic, succinic, formic, glycolic, acetic and maleic acid) were measured by means of HPLC, as described by Montesantos at al. [6]. Pyrazines and pyridines in the aqueous effluent were quantitated by means of DCM extraction followed by GC-MS. A liquid solution of 2-bromopyridine (250 mg/L) in DCM was used in all the extractions, which were performed with a solvent to feed ratio of 5 (volume basis). The GC-MS setup and GC program are described elsewhere [6]. Sulfate (SO₄²⁻), nitrate (NO₃⁻) and nitrite (NO₂) were quantitated with ion chromatography (IC) following the procedure reported by Montesantos et al. [6]. Conductivity of both the feeds and of the liquid effluents was measured offline, with a laboratory conductivity cell (Hach Lange Intellical CDC401). The composition of the SUS feeds was determined by means of ¹³C-Nuclear Magnetic Resonance (¹³C NMR), according to a procedure that will be reported in a future publication.

The gas phase, after the depressurization, was analyzed by means of a flue gas analyzer (Testo 340), with a percentage uncertainty of 10 % of the measured value for CO, SO₂ and NO₂, and 0.20 % for O₂. The gas samples collected in the gas bags were shipped to the Danish Technological Institute (TI) where proton-transfer-reaction mass spectrometry (PTR-MS) was used to measure Volatile Organic Compounds (VOC) and hydrogen sulfide (H₂S), both with a percentage uncertainty of 20 %.

Furthermore, TI used Cavity Ring-Down Spectroscopy (CRDS) to measure carbon dioxide (CO₂), nitrous oxide (N₂O) and ammonia (NH $_3$) concentrations with a percentage uncertainty of 10 %. Measurement methods were internally developed by TI.

2.4. Reduction of key overall quantities and elemental-based yields

The COD, TOC, and TN reductions (COD,, TOC,, TN,) for each test were calculated as:

$$P_r = \left(1 - \frac{X_{eff}}{X_0}\right) \bullet 100$$

where P_r represents the percentage reduction for COD, TOC, or TN, and $X_{\rm eff}$ and X_0 are the corresponding values of the quantity under investigation in the liquid effluent and the feed, respectively.

The elemental-based yields (Y_{ZW}) were defined as the mass flow rate of a specific element Z (i.e., carbon or nitrogen) belonging to a certain group of chemical species W in the liquid effluent over the mass flow rate of organic carbon or nitrogen fed to the system.

2.5. Ecotoxicity of SUS and HTO effluents

Ecotoxicological tests were conducted on selected HTO effluents (R4 – R6, R8 – R14: see Section 3.2) on two regulatory relevant marine test species: bacteria (Aliivibrio fischeri, formerly Vibrio fischeri) and algae (Skeletonema pseudocostatum). These two species were selected since they are the two OSPAR recommended test species, thereby ensuring a robust, regulatory-relevant approach to ranking of the treatment efficiencies. These species were also used in a previous study [14].

Inhibition of luminescence in *A. fischeri* was determined according to ISO 11348–3 with few modifications using freeze dried bacteria (ABOATOX, Finland). A concentration series was prepared following a two-fold dilution with 2 % saltwater from 0.125 % to 50 % (v/v), with exception of the reactor feeds tested in the range from 0.03125 % to 1 % (v/v). Bacterial luminescence after 15- and 30-min exposure was measured with Luminoskan TL Plus (Thermo Labsystem). The reference chemical 3,5-dichlorophenol was used to determine the validity of the test. Results were considered valid if the parallel controls did not deviate more than 3 % and exposure to 3.4 mg/L resulted in 20 % - 80 % inhibition of luminescence.

The marine algae S. pseudocostatum (NIVA-BAC 1, NIVA, Norway) were cultivated and maintained at DTU Sustain (Kgs. Lyngby, Denmark). The algal growth inhibition test was determined with a modified ISO 10253 utilizing in vitro fluorescence to quantify the biomass after acetone extraction [26]. Test concentrations were prepared in the range from 0.0625% to 1%(v/v), with exception of the reactor feeds tested in the range from 0.0003125 % to 0.01 % (v/v). The test was carried out with exponentially growing algal cultures inoculated at an initial cell density of 1·10⁵ cells/mL in 4 mL and incubated in 20 mL scintillation vials on an orbital shaker (IKA® Schüttler MTS 4) illuminated from below with fluorescent tubes (30 W/33; Philips, Amsterdam, The Netherlands). Quantification of biomass was done at 0 and 72 h by sampling 0.4 mL extracted with 1.6 mL acetone. Fluorescence of the extracts were used as a surrogate for biomass [26]. Effect concentrations and corresponding 95 % confidence intervals for the ecotoxicological tests were estimated using a log-normal function in GraphPad Prism (version 10.3.0). Conversion to the toxic units (TU) were done as TU = $100/EC_{50}$, where EC_{50} is the effect concentration of a test substance that causes 50 % of the maximum observed effect in a test organism. Further details on the analytical procedure, for both marine bacteria and algae, are reported elsewhere [14].

3. Results and discussion

3.1. SUS and SUS-derived samples

The physicochemical properties of the feed samples are reported in Table 1. The differences in TN, TS, COD, TOC and TIC between SUS A and SUS B, as well as the differences in the concentration of the H₂S scavenging related species (HET, TDZ, DTZ, MEA), underline the importance of considering the variability of the SUS, even when they are collected from the same offshore process lines. These variations can be attributed to various factors, such as fluctuation in the offshore process parameters, variations in the excess of HET injected during the scavenging process, temporary shutdown of some gas feed lines, etc. More specifically, the higher TN/TS value of SUS B (4.0) compared to SUS A (1.4) indicates a lower degree spent of SUS B, while the lower concentrations of C and N of SUS A indicate a higher degree of dilution with water of SUS A, presumably due to water condensation from the wet gas in contact with the scavenger. Even though the carbon is mainly in organic form, TIC accounts for 8.2 % and 3.3 % of TC for SUS A and SUS B, respectively. This is due to carbon dioxide co-absorption together with H₂S during the scavenging process of the produced gas. At the pH of the SUS samples (8.9), carbonate and mainly bicarbonate ions are

The COD of SUS A and SUS B is higher than the COD values typically encountered in current industrial applications of Wet Oxidation (e.g., 20 – 200 g/L [15]), while the COD of SUS A-P and SUS B-P is within or close to this range. As can be seen from Table 1, after the membrane separation the concentration of HET in the permeates (SUS A-P and SUS B-P) is approximately half of that in the feeds (SUS A and SUS B). TDZ and MEA concentrations are also reduced, albeit to a slight extent, whereas DTZ is not retained, thus showing approximately the same concentration in the permeates. As a result, TN is reduced more than TS, thereby the TN/TS ratio is reduced from 1.4 to 1.1 for SUS A, and from 4.0 to 2.4 for SUS B.

The discrepancy between the calculated TOC, TN, TS values, based on the molecular formula of HET, TDZ, DTZ, and MEA, and the experimental TOC, TN, TS, was calculated and percentage deviations were referred to the experimental values. The calculated TOC is within $-7\,\%$ and $+\,11\,\%$ of the experimental values, except for SUS A-P where the calculated carbon is overestimated (+42 %). The calculated TN is within $-24\,\%$ and $+\,30\,\%$, except for SUS A-P where the calculated nitrogen is overestimated (+41 %). The calculated sulfur is within $-17\,\%$ and $+\,22\,\%$, which is in line with the percentage uncertainty of the TS measurements (20 %). Overall, the data are in reasonable agreement,

Table 1Physicochemical properties of the SUS feeds. The uncertainty of all quantities, except TS, is reported as standard deviation of triplicate measurements. The uncertainty of the TS measurements is reported as provided by Eurofins.

Quantity	Units	SUS A	SUS A - P	SUS B	SUS B - P
TN	g/L	25 ± 2	14 ± 1	44 ± 2	24 ± 2
TS	g/L	18 ± 3	13 ± 2	11 ± 2	10 ± 2
COD	g/L	254 ± 5	138 ± 4	317 ± 5	212 ± 3
TOC	g/L	76 ± 2	37 ± 3	94 ± 2	60 ± 3
TIC	g/L	6.8 ± 0.3	2.1 ± 0.1	3.2 ± 0.2	$\textbf{2.4} \pm \textbf{0.1}$
HET	g/L	109.2	48.4	128.8	73.2
		± 1.4	$\pm~2.7$	\pm 3.5	\pm 4.3
TDZ	g/L	26.6	21.2	28.3	24.7
		$\pm~0.5$	$\pm~1.2$	± 1.0	\pm 1.7
DTZ	g/L	27.1	31.8	14.5	14.5
		± 0.1	$\pm \ 2.1$	± 0.3	± 0.5
MEA	g/L	23.5	20.2	15.2	11.8
		$\pm~0.7$	$\pm~0.8$	± 0.5	± 0.9
Conductivity	mS/	11.6	7.9	7.0	6.7
	cm				
pН	-	8.9	9.2	8.9	9.0
Density (at 21.5 °C)	kg/m ³	1042 ± 1	1033 ± 2	1085 ± 1	1063 ± 1

which implies that these four species account for most of the TOC, TN and TS.

3.2. HTO parameters and trends of overall quantities

3.2.1. HTO parameters

Experimental data of 14 HTO experiments are reported in Table 2. Four different feeds were used (SUS A, SUS B, SUS A-P and SUS B-P, see Fig. 2), with a feed COD (COD₀) in the range of 27-168 g/L, and two feed pH levels: natural (approximately 9) and high (approximately 13). All experimental runs were carried out under excess of oxygen, as expressed by the ratio of the oxygen supply (OS: molar flow rate of oxygen fed to the reactor) to the oxygen demand (OD: minimum molar flow rate of oxygen that is needed for the complete oxidation of the feed calculated based on COD₀). The ratio of the oxygen supply (OS) to the oxygen demand (OD), i.e., OS/OD, was in the range 1.13-1.35.

The first set of experiments (R1 – R7) was run on the natural SUS samples (i.e., SUS A and SUS B at their natural pH) and was focused on the variation of the feed COD, which was obtained by different dilution factors. In the couple of runs R2-R3 and R10-R11, the system was stabilized under nearly identical conditions, which was used for verifying the reproducibility of the experimental procedure. In addition, R7 was conducted at a slightly higher temperature, closer to the critical point of water. One of the main targets of this set of experiments was to determine the maximum feed COD level at which it was possible to keep the temperature at the desired subcritical value and to operate the HTO reactor under stable conditions. Besides the experiments reported in Table 2, some preliminary runs were also executed. One preliminary test, with COD₀ of ca. 200 g/L, faced challenges in maintaining the reactor temperature under control at subcritical values due to the excessive heat power generated by the reactions. Overall, feed COD values of about 130 - 170 g/L and reactor temperatures of about 325-335 °C were deemed optimal with the given setup. At these conditions, the reaction kinetics was high enough to guarantee substantial COD reductions (91 %-99 %) with reasonable residence times of the reacting mixture (τ) in the reactor (9–13 min), thus promising for the design of a compact offshore reactor for on-site treatment of the SUS.

In the outlet gas from experiments R4 and R5, high CO levels were detected (see Section 3.5). Two tests (R8, R9) were executed on the SUS samples (SUS A and SUS B) to investigate the influence of pH on the HTO process. This was done by the addition of a 50 wt% sodium hydroxide solution, in quantities calculated based on the TS contents of the feed with the aim of neutralizing any sulfuric acid that could have been formed. Since SUS A and SUS B were no longer available in sufficient quantity, another set of experiments (R10–R14) was conducted using the membrane permeates (SUS A-P or SUS B-P), i.e., the spent

scavengers. In addition, in another preliminary run with SUS A-P (not reported in Table 2: COD $_0$ 31 g/L and 325 °C) a significant pH drop to approximately 3 was observed before the steady state was reached. For this reason, it was deemed necessary to increase the feed pH for all permeates. A further consequence of the increased feed pH that was observed was the reduction of the CO levels in the outlet gas (see Section 3.5). This additional set of experiments (R10 – R14) was executed at approximately constant feed COD, which was set around 130 – 140 g/L in order to use SUS A-P without dilution, while SUS B-P was diluted in order to match the target value. The values of the feed COD for SUS A-P (R12, R13, R14) reported in Table 2 vary slightly, since the COD was remeasured before each individual execution of the HTO experiment, thus reflecting typical variations due to experimental uncertainties.

The operating pressure of the reactor was kept at approximately 24 MPa in all runs. Reactor temperatures in the tests were mostly 325 $^{\circ}$ C, except for four tests at 335 $^{\circ}$ C (R6, R8, R9, R14) and a single test at 350 $^{\circ}$ C (R7). The reactor temperatures (T) indicated in Table 2 represent the average of the reactor outside wall temperatures measured by the three thermocouples (T1, T2, and T3) along the reactor (see Fig. 3) in each test. These three temperatures were, however, approximately the same in all runs, as shown in the example of Fig. 4. The flow rate of the diluted SUS fed to the reactor was in the range 0.48–0.65 L/h, while the flow rate of the oxygen-enriched air was in the range 59–281 NL/h.

Fig. 5 shows the liquid effluents obtained in each test. Except for R1 and R7, characterized by low values of the feed COD, and R6, which was conducted at higher temperature, the effluents obtained from the HTO process with feeds at unaltered pH exhibited a yellowish color. On the other hand, when the feed pH was increased (R8 - R14), the HTO process yielded transparent effluents.

3.2.2. pH trends and operability

The pH of the effluents was always lower than the pH of the feed, as customary in HTO processes. As can be seen from Table 2, the pH of the liquid effluent (pHeff) was not affected significantly by the feed pH, with values in the range 6.9–8.1 for feeds with pH values around 9, and values consistently around 7.8 – 8.0 for feeds with pH values around 13. The perusal of Table 2 also shows that the pH of the effluents was significantly lower for feeds with low COD values (6.9 and 7.2 for R1 and R7, respectively), while it was always between 7.7 and 8.1 for all the other runs, which were characterized by COD $_0$ of at least 100 g/L and TOC $_0$ of at least 30 g/L, irrespectively of the initial pH. Furthermore, a large pH drop was observed in the previously mentioned preliminary run with SUS A-P feed and low feed COD (COD $_0$ 31 g/L and lower TN compared to SUS A). These experimental observations can be explained by the larger buffer capacity available for feeds with higher TOC and TN, as the oxidation reactions produce carbonates and ammonium (see

Table 2
Operating conditions for the HTO reactor for each test, pH of the effluent, and COD and TOC percentage reduction between feed and effluent. T: reactor outside wall temperature; pH₀: feed pH; OS/OD: ratio of the oxygen supply to the oxygen demand; COD₀: feed COD; TOC₀: feed TOC; τ: residence time of the reacting phase in the HTO reactor; pH_{eff}: pH of the liquid effluent; COD_r: Chemical Oxygen Demand reduction; TOC_r: Total Organic Carbon reduction.

Run	SUS	pH_0	T	SUS Flow Rate	Oxygen - Enriched Air Flow Rate	OS/OD	COD_0	TOC_0	τ	pH_{eff}	COD_r	TOC_r
(#)	(type)	(-)	(°C)	(L/h)	(NL/h)	(-)	(g/L)	(g/L)	(min)	(-)	(%)	(%)
R1	A	9.1	325	0.48	59.4	1.18	27	8.0	23	6.9	93	87
R2	Α	9.1	325	0.54	178.2	1.22	101	30.0	14	7.7	95	91
R3	A	9.1	325	0.60	183.6	1.28	105	31.1	13	7.7	95	91
R4	В	9.1	325	0.62	178.2	1.23	101	30.9	13	7.8	96	93
R5	В	8.9	325	0.61	252.0	1.28	132	40.4	11	8.0	96	92
R6	В	9.1	335	0.64	280.8	1.17	165	50.5	9	8.1	97	96
R7	Α	9.1	350	0.60	69.6	1.20	32	9.6	19	7.2	93	91
R8	A	12.9	335	0.58	243.0	1.39	149	44.1	11	7.8	99	98
R9	В	12.9	335	0.58	232.2	1.22	168	51.4	11	8.0	99	100
R10	B - P	12.9	325	0.57	189.0	1.29	128	39.0	13	7.9	94	91
R11	B - P	12.9	325	0.60	189.0	1.24	130	39.6	13	7.9	94	91
R12	A - P	13.0	325	0.60	226.8	1.35	139	37.0	11	7.9	96	93
R13	A - P	13.0	325	0.65	178.2	1.17	126	33.5	13	8.0	91	86
R14	A - P	13.0	335	0.61	194.4	1.13	143	38.0	13	8.0	95	93

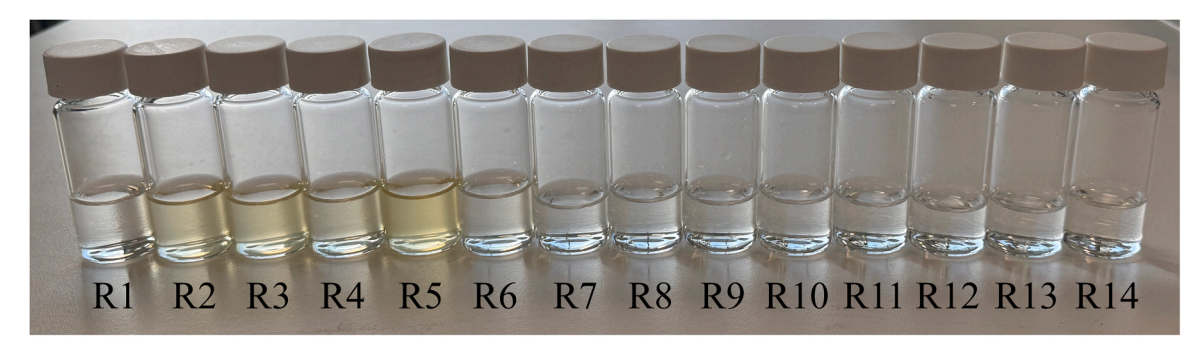


Fig. 5. Liquid effluents from all the experimental runs. The corresponding run number if reported.

Section 3.3). The presence of carbonate/bicarbonate/carbonic acid equilibria (pKa of carbonic acid and bicarbonate 6.4 and 10.3 at 25 °C, respectively [27]) and the presence of the ammonium/ammonia equilibria (pKa of ammonium 9.25 at 25 °C [27]) provide buffer capacity, which is larger at higher concentrations of carbon and nitrogen in the feed. The presence of such a buffer capacity is a key aspect, since it avoids the pH to drop substantially, thereby avoiding the formation of sulfuric acid, which is corrosive. This observation indicates that conducting the hydrothermal oxidation of the SUS at relatively high feed COD, i.e., without dilution of the feed or at moderate dilution levels, is positive both with respect to saving dilution water and to minimizing the reactor volume, as well as safeguarding the reactor integrity, provided that the heat removal rate is sufficient to keep the reactor temperature under control within the subcritical water range.

During the reactor shutdown in one of the preliminary tests, the pH decreased rapidly to 2.1 (see Fig. 6), even though the pH was rather stable during the operation at steady state. A possible explanation of the observed phenomenon is connected to ammonia stripping. During the shutdown, water is fed to the system instead of SUS feed, thereby stopping the continuous addition of carbonate- and ammonium-forming species and reducing the buffer capacity of the aqueous phase inside the reactor, while enriched-oxygen air continues to flow into the reactor. The gas flow must strip ammonia from the aqueous phase, causing the shift of the ammonium/ammonia equilibrium towards ammonia and H_3O^+ :

$$NH_{4(aq)}^{+} + H_{2}O_{(l)} \quad \rightleftarrows NH_{3(aq)} + H_{3}O_{(aq)}^{+}$$

This reduces the overall buffer capacity of the solution and shifts the carbonate equilibrium away from bicarbonate/carbonate pair toward the bicarbonate/carbonic acid pair. As a result, increased $\rm CO_2$ outgassing occurs, shifting the equilibrium. Once pH reached 2.1 in this preliminary run, sodium hydroxide was added to the system to prevent the risk of corrosion, and high pH values were established. To avoid this issue in other tests, the use of a sodium hydroxide solution, instead of

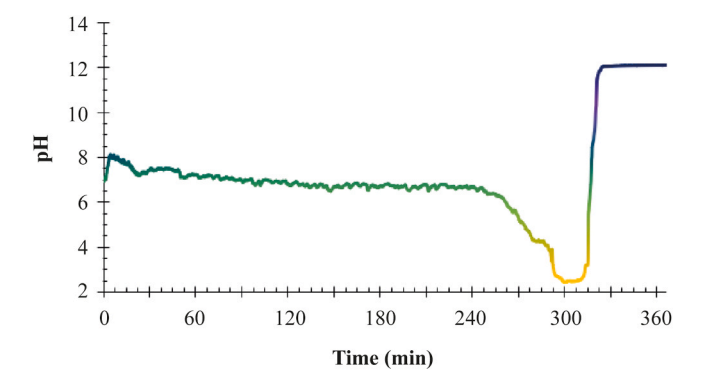


Fig. 6. pH trend during HTO operation at steady-state and during shutdown in a preliminary test.

demineralized water, was implemented during the shutdown in all experimental runs (see Section 2.2).

3.2.3. COD and TOC reductions

As can be seen in Table 2 and Fig. 7, the COD and TOC of the SUS were successfully reduced by at least 91 % and 86 %, respectively, under all conditions investigated. The reduction of these two quantities was particularly high in R8 and R9, which were characterized by high reactor temperature (335 °C), high feed pH (12.9) and high excess of oxygen (OS/OD 1.26 and 1.32). The combination of these factors, or some of them, is the probable reason for the almost complete removal of the organics in the effluent, which was obtained with two different feeds (SUS A and SUS B). Within the ranges under investigation, the increase in pH is believed to have the most significant influence on the removal efficiency of COD and TOC compared to the temperature increase and oxygen excess. This is evident when comparing the alkaline experiments R8 and R9 to other high-temperature runs (335 °C and 350 °C) conducted at the natural pH of the SUS and with similar or lower initial COD levels, such as R6 and R7. Additionally, a preliminary run at 335 $^{\circ}\text{C}$ with a high initial COD (160 g/L) and elevated oxygen excess (OS/OD = 1.71) achieved a COD removal efficiency of only 93 %, while R6 and R7 yielded 93-97 %, with the highest-temperature condition (R7) performing the worst. In contrast, the alkaline runs (R8 and R9) achieved COD removal efficiencies of 99 %, underscoring the enhanced effectiveness of an alkaline environment for organic degradation. However, overall, the results indicate that the HTO process is quite versatile with respect to the feed composition and is similarly effective at almost all the conditions investigated.

The tests conducted in this work in a continuous-flow reactor are in qualitative agreement with the results obtained in a laboratory batch reactor reported elsewhere [6,14], where reaction times of 20 min were required to achieve more than 90 % COD reduction at 350 °C. In all the tests in continuous-flow mode the TOC was reduced more than 86 %, while in batch-mode 40 min were necessary to achieve a TOC reduction of more than 80 % [6]. The continuous-flow reactor is seemingly more efficient, likely due to better phase mixing and the absence of stirring limitations inherent in the HTO batch reactor, leading to higher contact area between the gas and the liquid phase and, therefore, higher rates of oxygen transfer from the gas to the liquid. It is also noted that the reactor temperatures reported in this work are wall temperatures, while the temperatures measured in the abovementioned works [6,14] were measured in the bulk of the liquid phase. Therefore, any direct comparison must be made with caution.

3.2.4. TN reduction

The Total Nitrogen reduction (TN_r) data are reported in the Supplementary Information (Table S2). As can be seen, TN_r is observed in the range 6–68 %. A reduction in TN suggests that some of the nitrogen is transformed into nitrogen gas (N_2) via ammonium/ammonia. Ammonium prevails as the primary form in the ammonium-ammonia equilibrium (see Table S2 in the Supplementary Information), as the

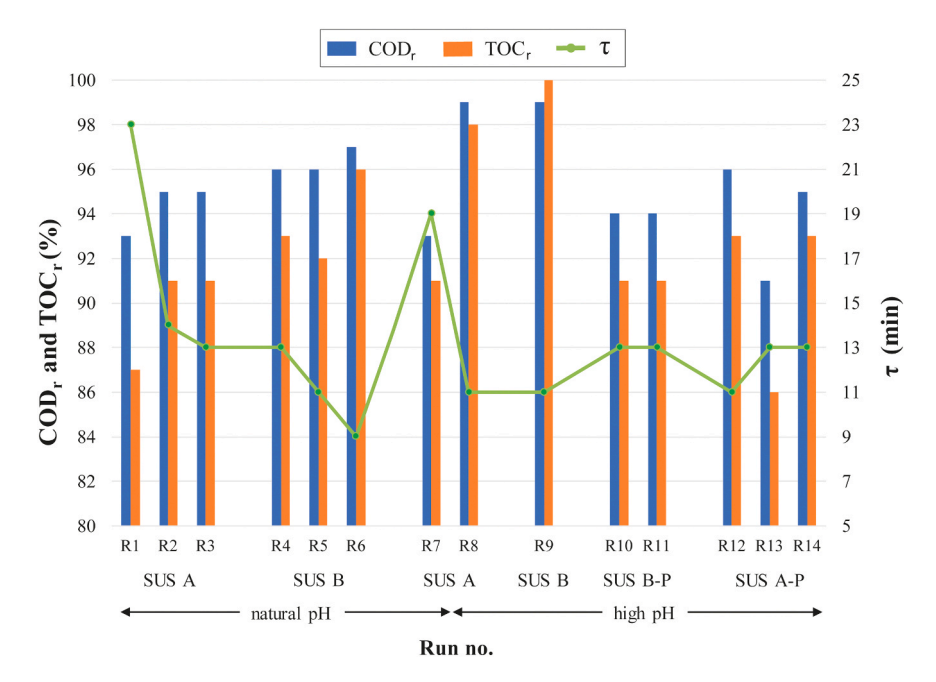


Fig. 7. COD and TOC percentage reduction (left axis) with corresponding residence time (right axis) for each run.

liquid effluents exhibited pH $_{\rm eff}$ levels between 6.9 and 8.1. To accommodate Le Chatelier's principle, ammonia must distribute between the aqueous and the gas phase, thereby causing the conversion of ammonium ions to ammonia in the aqueous phase. In gas phase, ammonia is oxidized to nitrogen gas even without a catalyst [28], which explains the very low levels of ammonia in the gas effluent (always lower than 39 ppmv), as also noted in Section 3.5. TN_r appears to be influenced by the TN content of the feed. The larger TN_r values (36–68 %) were obtained on SUS B (TN 44 g/L), while TN_r values in the range 13–44 % and 19–30 % were observed on SUS A (TN 25 g/L) and SUS B-P (TN 24 g/L), respectively, and the smaller TN_r values (6–22 %) were observed on SUS A-P (TN 14 g/L).

3.3. Composition of the liquid effluents

Ammonium, nitrate, sulfate, short-chain carboxylic acids, pyrazines and pyridines were observed in all effluents. However, their concentrations and relative amounts varied among the different liquid effluents. Ammonium is strongly favored over nitrate, with concentrations in the range 2.1 g/L to 18 g/L and 0.002 g/L to 1.8 g/L, respectively. The sulfate concentration ranged from 2.9 g/L to 19 g/L, expect in R6, R8 and R9, which exhibited significant sulfur balance discrepancies, as discussed later.

Except for R9, which was characterized by complete removal of organic carbon (see Table 2), short-chain carboxylic acids (i.e., acetic, formic, glycolic, maleic, oxalic and succinic acid) were detected and quantified in each test. Excluding R9, acetic acid was consistently largely predominant with concentrations ranging from 0.8 g/L to 7.4 g/ L, while formic, glycolic and succinic acid were in the range of 0-1.2 g/ L, 0 - 0.56 g/L and 0 - 0.28 g/L, respectively. Oxalic and maleic acids were found only in one run at ppm levels (≤ 0.01 g/L). Pyrazine and pyridine, as well as their alkyl-derivates (i.e., methyl-pyrazine, 2,3dimethyl-pyrazine, 3-methyl-pyridine, and 2,5-dimethyl-pyridine), hereafter referred to as pyrazines and pyridines, were also identified in the liquid effluent. Pyrazine, pyridine, and 3-methyl-pyridine were the most abundant, with concentrations in the range of 0.01 - 0.30 g/L, $0.08-0.82\ g/L$ and $0.01-0.21\ g/L,$ respectively, whereas the concentration trations of 2,3-dimethyl-pyrazine, methyl-pyrazine, and 2,5-dimethylpyridine never exceeded 0.06 g/L. Concentrations of the identified species in all runs are reported in Table S3 and Table S4 in the

Supplementary Information.

Previous research work [6,14] showed that HET, DTZ, and MEA are not observed in the HTO effluent even at lower temperatures and lower reaction times, compared to the values of this work. In other words, they degrade very fast and are not observed in the effluent. In addition, it is known that HET hydrolyzes at pH values below 9 (even at room temperature) or high temperature, with the decomposition rate increasing with lowering pH and with increasing temperature. At pH 8 and 333 K the half-life of HET was measured to be far less than one second [7]. It is therefore deemed probable that HET, and similarly TDZ and DTZ, quickly releases MEA under HTO conditions. MEA is then converted to simple carboxylic acids (e.g., glycolic, formic, acetic) and ammonium/ammonia [29,30], as well as pyrazines and pyridines [31,32]. Experimental evidence on sulfur oxidation intermediates is not available, but it can be hypothesized that the ring-opening reactions of TDZ and DTZ release methanethiol, which in turn can be oxidized to SO₂, sulfite and eventually sulfate [33].

The organic species that were identified account for 62--103~% of the TOC of the liquid effluents, except for R9 where no residual TOC was found in the effluent. Regarding the nitrogen-containing molecules, the identified species account for more than 71 % of the total nitrogen in the liquid effluent, with ammonium being the most abundant species which was always above 68~%. Regarding the sulfur-containing species, sulfate constitutes 76--116~% of the total sulfur in the liquid effluent, confirming that it is the dominant sulfur-containing species in the HTO process [6, 22]. Values exceeding 100~% may reflect discrepancies between ICP (for TS) and IC (for sulfate) measurements.

The sulfur balance did not close well in several cases. More specifically, the sulfur recovered in the effluents was from 29 % to 64 % lower than the sulfur at inlet in all runs, except for R6, R8, and R9, where the sulfur at the outlet was basically unrecovered (96–99.9 % lower than the sulfur at inlet, as reported in Table S5 in the Supplementary Information). Since sulfur was only detected at trace levels in the gas phase (see Section 3.5) and no sulfur species other than sulfate were detected, which is consistent with literature findings [22], the reactor was disassembled and inspected in between some of the runs to search for sulfur-rich solid deposits. Solid deposits inside the reactor were not found. However, fine solid particles were sometimes observed in the wash water, i.e., the water collected in the shutdown phase. We deem that the missing sulfate in the liquid effluents during steady state

operation is due to precipitation and consequent accumulation of sulfate salts inside the reactor, followed by subsequent re-dissolution of those salts during the shutdown procedure. During HTO, sulfate salts form in the liquid phase, with their solubility depending on the operating conditions. It is known that the solubility of sulfate salts drops at near-critical conditions. For example, Dipippo et al. [34] reported that the solubility of sodium sulfate drops substantially at near-critical conditions (320 - 365 °C). It is noted that the three runs with almost no sulfur recovered in the effluent (i.e., R6, R8, and R9) were characterized by both higher temperature (reactor outside wall temperature of 335 °C, instead of 325 °C applied in most of the runs) and high feed concentration (COD₀ in the range 149–168 g/L). These two factors must have contributed to high temperatures and high sulfate concentrations in the core of the reactor, thus leading to sulfate accumulation and possibly precipitation. Therefore, it is possible that the sulfur that dropped out inside the HTO reactor during the operation at steady state was re-dissolved during the shutdown phase, when sulfate production ceases, demineralized water is fed to the system, the temperature is reduced and, therefore, the sulfur salts are re-dissolved, or partially re-dissolved leading to fine particles that can be entrained in the wash water flow, and carried over in the wash water. In one case (R6) the wash water was analyzed, and a high quantity of sulfate (55.5 g/L) was found. This observation supports the hypothesized mechanism of sulfur dropout and accumulation at the reactor conditions, followed by re-dissolution in the wash water during the shutdown. These observations regarding the sulfur balance suggests limiting the reactor wall temperatures to 325 °C as in long term operation at steady state sulfur precipitation may represent a fouling operational issue. This aspect would require further investigation in the demonstration of the technology for longer operational times.

3.4. Elemental-based yields

The carbon-based and nitrogen-based yields of key chemical species formed in the oxidation process were calculated, according to the definition reported in Section 2.4. The carbon-based yield of carboxylic acids (Y_{CA}) was in the range 0–10 %, with acetic acid identified as the dominant compound (see Section 3.3), which is in line with the higher stability of this compound as supported by the higher temperatures required for its degradation [35]. The carbon-based yield of pyrazines and pyridines (Y_{CP}) was in the range 1.0–2.4 % in the experimental runs at natural pH (R1 – R7), while lower values (i.e., 0.5 %–0.9 %) were

found at higher feed pH with all the four types of feed (R8 – R14). This suggests that higher pH values lead to faster decomposition of pyrazines and pyridines. Complete data of Y_{CA} and Y_{CP} , as well as their ratio, are reported in Table S6 in Supplementary Information.

The values of Y_{CA} and Y_{CP} are in line with the findings of Montesantos et al. [6]. Regarding these intermediate oxidation products, the lower maximum concentrations and yields of pyrazines and pyridines vs carboxylic acids indicate that the former compounds decompose faster than carboxylic acids. It is however remarked that in R8 and R9, as noted in Section 3.2.3, basically all organics are converted and removed from the liquid effluent, indicating that also carboxylic acids decompose in relatively short reaction time (11 min) at relatively high reactor temperature (335 °C), high pH and high OS/OD.

As can be seen from Fig. 8, ammonium consistently stands out as the dominant nitrogen-based compound, with nitrogen-based yields (Y_{NA}) ranging from 24 % to 87 %. The nitrogen-based yields of pyrazine and pyridines (Y_{NP}) account for 0.3–1.8 %, whereas the yield of nitrate (Y_{NN}) ranges from 0.002 % to 2.80 %. The direct comparison of the results of R6 and R9 (both SUS B, similar operating conditions but different feed pH) further supports the hypothesis that high feed pH, as discussed above, favors the decomposition of pyrazines and pyridines. In addition, a slightly higher formation of nitrates is observed in tests at higher feed pH. Y_{NA} , Y_{NP} , Y_{NN} values for each test are reported in Table S7 in Supplementary Information.

3.5. Composition of the gas effluents

Gas sampling was conducted for tests R4, R5, R6 and from R8 to R14. In the tests R4, R5 and R6, with feed pH \leq 9.1, carbon monoxide (CO) was observed at concentrations in the range 5900–7300 ppmv. When the pH values of the feed were significantly increased (R8 – R14), CO concentrations were drastically reduced, and they were observed in the range 480–920 ppmv. Additionally, the concentrations of NH₃, N₂O, NO₂, H₂S, and SO₂ were measured. Specifically, NH₃, N₂O, NO₂, and SO₂ exhibited a maximum concentration of a few ppmv (\leq 39 ppmv).

Regarding H_2S , it was only observed in the runs with SUS A-P (R12, R13, R14), with a maximum concentration of 0.6 ppm. SUS A-P is characterized by the lowest TN/TS ratio among the tested feeds, which can contribute to H_2S . The presence of the said small concentrations of H_2S may be explained by the decomposition of organosulfur compounds in the absence of oxygen, which may be caused by the occurrence of localized regions in the reactor with limited oxygen availability due to

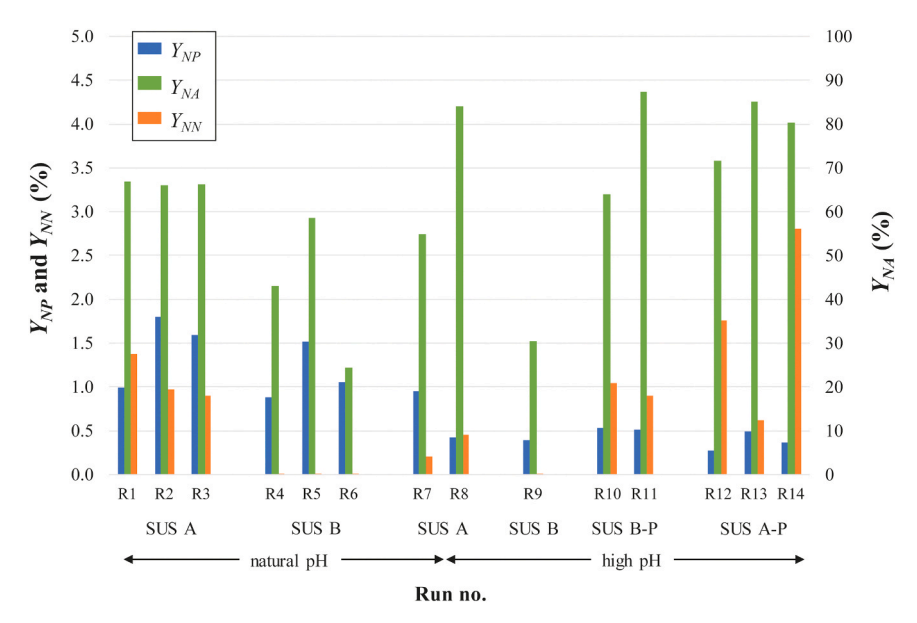


Fig. 8. Nitrogen-based yield of pyrazines–pyridines (Y_{NP}) and nitrate (Y_{NN}) on the left axis. Nitrogen-based yield of ammonium (Y_{NA}) on the right axis.

mass-transfer limitations in the two-phase reacting system (subcritical water + gas). The $\rm H_2S$ formation during the SUS A-P tests would need further investigation and parameter optimization to determine the best measure to ensure no $\rm H_2S$ is produced by suboptimal oxidation for the low TN/TS ratio feeds. The data from all the measurements are reported in Table S8 in the Supplementary Information.

Following the DIRECTIVE 2010/75/EU, for combustion plants firing natural gas using gas engines, CO emissions must be below 100 mg/Nm² (ca. 87 ppm). In our study, the concentration of CO in the gas effluent is over the limit and therefore the gas effluent cannot be vented. However, since the flow rate of the HTO gas effluent is about five orders of magnitude lower than the flow rate of the produced gas, the HTO gas effluent could be directly mixed with the produced gas without affecting the composition of the export gas, since the CO would be diluted at partper-billion (ppb) levels. CO is not explicitly regulated in EU and international pipeline transmission standards (e.g., EN 16726, ISO 13686) and at ppb-levels it is not expected to pose any technical concern. The extensive dilution of the HTO gas effluent in the natural gas pipeline (i. e., in the order of 10^5 times) would also bring CO_2 and the residual O_2 , present due to the small excess of oxygen used in the HTO, at levels well below the maximum allowable limits, which, according to the EN 16726 standard, are 2.5 mol% for CO2 and 0.001 mol% for O2.

3.6. Ecotoxicity of SUS and HTO effluents

Ecotoxicological tests were conducted for runs R4 – R6 and R8 – R14. Reference tests with 3,5-dicholorphenol resulted in EC50 values of 1.2 mg/L $[0.72-1.7]_{95\%}$ confidence interval for *S. pseudocostatum* and *A. fischeri* exposed to 3.4 mg/L 3,5-dichlorophenol resulted in 33 % luminescence inhibition. Both values are within the expected range for the reference substance according to ring-tests following standardized guidelines (ISO, 11348–3:2007; ISO, 10253:2016). Fig. 9 shows the residual TU for the SUS after treatment with different operating conditions of the HTO reactor according to Table 2. The TU for the feed prior to treatment for *A. fischeri* resulted in 2500 TU and 1350 TU for SUS A and SUS B, respectively, while exposure to *S. pseudocostatum* resulted in TU of 29400 and 17000 for SUS A and SUS B, respectively. The values are within the range of previously tested SUS [14]. All tested operating

conditions resulted in > 99 % mitigation of the toxic response for *A. fischeri* for their respective feeds (here measured as decrease in TU compared to the reactor feed). Consequently, the initial difference in toxicity of the feed had no marked impact on the removal efficiency of toxicity for *A. fischeri*. EC₅₀ (*A. fischeri*) for test R9 could not be determined within the tested concentration range due to the absence of a clear concentration-response relationship, making TU value unavailable. Across all operating conditions the residual toxicity was similar to currently observed toxicity values for PW discharges in the North Sea [36,37], bearing in mind that the SUS stream is a large contributor to the overall toxicity of PW. Consequently, by treatment of the SUS with HTO would have an expected decrease in the environmental impact factor of the PW by approximately 20 %, in cases such those reported by Stipanicev et al. [13].

The difference in sensitivity between A. fischeri and S. pseudocostatum by approximately a factor of 10–100 can largely be explained by the difference in endpoint observed, acute and chronic, respectively [38]. While the HTO treated SUS also resulted in a large relative decrease in toxicity towards S. pseudocostatum (94 %-98 %) across treatment and feed types, a marked absolute residual ecotoxicity in terms of TU remains. While there are multiple ways of investigating the residual matrix toxicity it was considered beyond the scope of this study. All the data for EC₅₀ and TU are available in the Supplementary Information in Table S9.

N/A: not available measurement, EC_{50} could not be established within the tested concentration range.

4. Conclusion

The operability of the hydrothermal oxidation of spent and unspent $\rm H_2S$ scavengers was proved in continuous-flow mode of operation for feed COD up to 168 g/L. Large reductions of the wastewater COD (91–99 %), TOC (86–100 %), and toxic response with respect to regulatory relevant marine bacteria (>99 %) and algae (94–98 %) were found. The reaction was autothermal and no external sources of heat were needed during steady state conditions. Nitrogen- and sulfurcontaining organic compounds were mostly converted to ammonium and sulfates, respectively. Most of the carbon was fully oxidized to

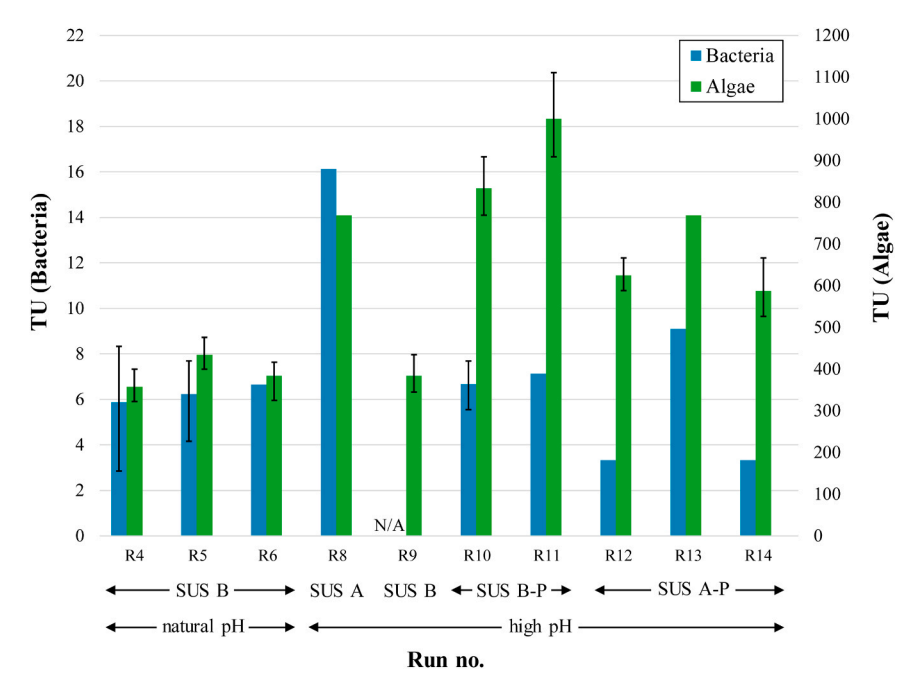


Fig. 9. Residual ecotoxicity of luminescence decrease using *Aliivibrio fischeri* after exposure to HTO effluents reported as Toxic Unit ($TU = 100/EC_{50}$), on the left axis. Residual ecotoxicity of growth inhibition using *Skeletonema pseudocostatum* after exposure to HTO effluents reported as Toxic Unit, on the right axis. Error bars represent the 95 % confidence interval of the fitted log-normal function.

carbon dioxide, with intermediate oxidation products in the liquid effluent mainly consisting in acetic acid (0.77-7.4 g/L) with very small amounts of other short-chain carboxylic acids (always lower than 1.6 g/ L in total), pyrazines (always lower than 0.5 g/L) and pyridines (always lower than 1.0 g/L). Carbon monoxide was also detected in the gas effluent, with concentrations around 5800-7200 ppm for natural feed pH, while values of one order of magnitude lower (in the range 480–920 ppm) were measured for high feed pH. The buffer capacity of the carbonate/bicarbonate/carbonic acid and ammonium/ammonia equilibria is crucial in preventing significant pH drops in the reactor. For feed COD and TOC values above 100 g/L and 30 g/L, respectively, the pH of the effluent was always observed between 7.7 and 8.1, which are safe values with respect to corrosion risk due to formation of sulfuric acid. The definition of the optimal SUS feed COD must take into account two different aspects: (i) High feed COD levels (e.g., above 100 g/L) provide buffer capacity and prevent substantial pH drop, therefore minimizing risks of corrosion of the reactor; (ii) At too high feed COD (e. g., 200 g/L) the continuous-flow HTO reactor could not be run at steady state in subcritical conditions, due to the excessive heat power generation. Therefore, the COD values for a prospective offshore implementation should be as high as possible, to provide buffer capacity and minimize the consumption of dilution water, subject to the maximum heat power removal that can be realized to keep the reactor under subcritical conditions and its volume as small as possible.

CRediT authorship contribution statement

Alessandro Perrucci: Writing - review & editing, Writing - original draft, Validation, Methodology, Investigation, Formal analysis, Data curation, Conceptualization. Sofie Askjær Hass: Writing - review & editing, Validation, Resources, Methodology, Investigation, Formal analysis, Data curation, Conceptualization. Maria Nymann Christensen: Writing - review & editing, Validation, Resources, Methodology, Investigation, Formal analysis, Data curation, Conceptualization. Lars Michael Skjolding: Writing - review & editing, Writing - original draft, Validation, Methodology, Investigation, Formal analysis, Data curation. Sarah Fredung Hückelkamp: Writing - review & editing, Validation, Resources, Methodology, Investigation, Formal analysis, Data curation, Conceptualization. Jens Muff: Writing - review & editing, Supervision, Funding acquisition. Marco Maschietti: Writing review & editing, Validation, Supervision, Resources, Project administration, Methodology, Investigation, Funding acquisition, Data curation, Conceptualization.

Declaration of Competing Interest

The authors declare that they have no known competing financial interests or personal relationships that could have appeared to influence the work reported in this paper.

Acknowledgments

This study was funded by the Danish Offshore Technology Center (DTU Offshore) as part of the program Produced Water Management. The authors are grateful to Benaiah Anabaraonye (DTU Offshore, program manager), Simon I. Andersen (DTU Offshore, research leader in Offshore Produced Water Management), Ole Andersen (DTU Offshore, surface engineer advisor), Charlotte Lassen (DTU Offshore, reservoir engineer advisor) and Yanina D. Ivanova (DTU Offshore, production chemistry advisor), for the continuous and valuable technical discussions carried out during the execution of this work. In addition, the authors are grateful to: Zhuoyan Cai (Aquarden Technology, CEO of Aquarden), for the insightful technical discussions; Alaa Khalil (Aalborg University) for producing the membrane permeates of spent and unspent scavengers; Linda B. Madsen (Aalborg University) for the execution of the total carbon and HPLC analysis; Dorte Spangsmark (Aalborg

University) for the execution of the ion chromatography analysis; Nicolai K. Nielsen (Aalborg University) for the development of gas chromatographic and mass spectrometric analytical methodologies.

Appendix A. Supporting information

Supplementary data associated with this article can be found in the online version at doi:10.1016/j.jece.2025.118881.

Data availability

Data will be made available on request.

References

- OSHA. Hydrogen Sulfide, (https://www.osha.gov/hydrogen-sulfide/hazards), 2024 (accessed April 15, 2024).
- [2] F. Pouliquen, C. Blanc, E. Arretz, I. Labat, J. Tournier-Lasserve, A. Ladousse, J. Nougayrede, G. Savin, R. Ivaldi, M. Nicolas, J. Fialaire, R. Millischer, C. Azema, L. Espagno, H. Hemmer, J. Perrot, Hydrogen sulfide, ullmann's encycl. Ind. Chem, Wiley-VCH Verlag GmbH & Co. KGaA, Weinheim, 2000, https://doi.org/10.1002/ 14356007.a13 467.
- [3] O.M. Suleimenov, R.E. Krupp, Solubility of hydrogen sulfide in pure water and in NaCl solutions, from 20 to 320°C and at saturation pressures, Geochim. Et. Cosmochim. Acta 58 (11) (1994) 2–48, https://doi.org/10.1016/0016-7037(94) 000221
- [4] S. Mokhatab, W.A. Poe, J.Y. Mak, Basic concepts of natural gas processing, in: Handbook of Natural Gas Transmission and Processing, fourth ed., Gulf Professional Publishing, 2019, pp. 177–189, https://doi.org/10.1016/B978-0-12-815817-3.00004-6.
- [5] M.A. Kelland, Hydrogen sulfide scavengers, in: Production Chemicals for the Oil and Gas Industry, second ed., CRC Press, 2014, pp. 353–368, https://doi.org/ 10.1201/b16648.
- [6] N. Montesantos, M.N. Fini, J. Muff, M. Maschietti, Proof of concept of hydrothermal oxidation for treatment of triazine-based spent and unspent H₂S scavengers from offshore oil and gas production, Chem. Eng. J. 427 (2022) 131020, https://doi.org/10.1016/j.cej.2021.131020.
- [7] J.M. Bakke, J. Buhaug, J. Riha, Hydrolysis of 1,3,5-tris(2-hydroxyethyl)hexahydro-s-triazine and its reaction with H₂S, Ind. Eng. Chem. Res. 40 (26) (2001) 6051–6054, https://doi.org/10.1021/ie010311y.
- [8] J.M. Bakke, J. Buhaug, Hydrogen sulfide scavenging by 1,3,5-Triazinanes. comparison of the rates of reaction, Ind. Eng. Chem. Res. 43 (9) (2004) 1962–1965, https://doi.org/10.1021/ie030510c.
- [9] I. Romero, F. Montero, S. Kucheryavskiy, R. Wimmer, A. Andreasen, M. Maschietti, Temperature- and pH-Dependent kinetics of the aqueous phase hydrogen sulfide scavenging reactions with MEA-Triazine, Ind. Eng. Chem. Res. 62 (21) (2023) 8269–8280, https://doi.org/10.1021/acs.iecr.3c00668.
- [10] I. Romero, S. Kucheryavskiy, M. Maschietti, Experimental study of the aqueous phase reaction of hydrogen sulfide with MEA-Triazine using in situ Raman spectroscopy, Ind. Eng. Chem. Res. 60 (43) (2021) 15549–15557, https://doi.org/ 10.1021/acs.iecr.1c03833.
- [11] J.J. Wylde, G.N. Taylor, K.S. Sorbie, W.N. Samaniego, Formation, chemical characterization and oxidative dissolution of amorphous polymeric dithiazine (apDTZ) during the use of the H₂S scavenger monoethanolamine-triazine, Energy Fuels 34 (8) (2020) 9923–9931, https://doi.org/10.1021/acs. energyfuels.0c01402.
- [12] M. Maschietti, A. Khalil, A. Perrucci, K. Szlek, S. Hückelkamp, S.A. Hass, M.N. Christensen, J. Muff, Resource recovery and environmental footprint reduction in H₂S scavenging of natural gas with MEA-triazine in offshore oil and gas production. In: Production Chemistry Symposium (2024), Geilo, 2024.
- [13] M. Stipanicev, Ø. Birketveit, V.H. Kvalheim, J. Hoshowski, M.G. Lioliou, T. Rindalsholt, Multifunctional H₂S scavenger and corrosion inhibitor: addressing integrity challenges and production output of the mature field, SPE- 190911-MS. Proceedings of the SPE International Oilfield Corrosion Conference and Exhibition, SPE International, Aberdeen, 2018, https://doi.org/10.2118/190911-MS.
- [14] N. Montesantos, L.M. Skjolding, A. Baun, J. Muff, M. Maschietti, Reducing the environmental impact of offshore H₂S scavenging wastewater via hydrothermal oxidation, Water Res 230 (2023) 119507, https://doi.org/10.1016/j. watres.2022.119507.
- [15] S.T. Kolaczkowski, P. Plucinski, F.J. Beltran, F.J. Rivas, D.B. McLurgh, Wet air oxidation: a review of process technologies and aspects in reactor design, Chem. Eng. J. 73 (2) (1999) 143–160, https://doi.org/10.1016/S1385-8947(99)00022-4.
- [16] M.J. Dietrich, T.L. Randall, P.J. Canney, Wet air oxidation of hazardous organics in wastewater, Environ. Prog. 4 (3) (1985) 171–177, https://doi.org/10.1002/ ep.670040312.
- [17] H. Debellefontaine, J.N. Foussard, Wet air oxidation for the treatment of industrial wastes. Chemical aspects, reactor design and industrial applications in Europe, Waste Manag 20 (1) (2000) 15–25, https://doi.org/10.1016/S0956-053X(99) 00306-2.
- [18] G. Brunner, Near and supercritical water. Part II: oxidative processes, J. Supercrit. Fluids 47 (3) (2009) 382–390, https://doi.org/10.1016/j.supflu.2008.09.001.

- [19] Z. Alipour, A. Azari, COD removal from industrial spent caustic wastewater: a review, J. Environ. Chem. Eng. 8 (3) (2020) 103678, https://doi.org/10.1016/j. iece 2020 103678
- [20] A. Tungler, E. Szabados, A.M. Hosseini, Wet Air Oxidation of Aqueous Wastes, In: Wastewater Treatment Engineering, (2015), pp. 153-169, https://doi.org/10.5 772/60935
- [21] H. Debellefontaine, S. Crispel, P. Reilhac, F. Perie, J.N. Foussard, Wet air oxidation (WAO) for the treatment of industrial wastewater and domestic sludge. Design of bubble column reactors, Chem. Eng. Sci. 54 (21) (1999) 4953–4959, https://doi. org/10.1016/S0009-2509(99)00217-1.
- [22] S.K. Bhargava, J. Tardio, J. Prasad, K. Foger, D.B. Akolekar, S.C. Grocott, Wet oxidation and catalytic wet oxidation, Ind. Eng. Chem. Res. 45 (4) (2006) 1221–1258, https://doi.org/10.1021/ie051059n.
- [23] M.N. Fini, N. Montesantos, M. Maschietti, J. Muff, Performance evaluation of membrane filtration for treatment of H₂S scavenging wastewater from offshore oil and gas production, Sep. Purif. Technol. 277 (2021) 119641, https://doi.org/ 10.1016/j.seppur.2021.119641.
- [24] A. Khalil, N. Montesantos, M. Maschietti, J. Muff, Facile fabrication of high-performance nanofiltration membranes for recovery of triazine-based chemicals used for H₂S scavenging, J. Environ. Chem. Eng. 10 (6) (2022) 108735, https://doi.org/10.1016/j.jece.2022.108735.
- [25] A. Khalil, M. Maschietti, J. Muff, Influence of graphene oxide additives on the NF separation of triazine-based H₂S scavenging compounds using advanced membrane technology, Chemosphere 360 (2024) 142439, https://doi.org/10.1016/j.chemosphere.2024.142439.
- [26] P. Mayer, R. Cuhel, N. Nyholm, A simple in vitro fluorescence method for biomass measurements in algal growth inhibition tests, Water Res 31 (10) (1997) 2525–2531, https://doi.org/10.1016/S0043-1354(97)00084-5.
- [27] W.M. Haynes, Section 5: thermochemistry, electrochemistry, and solution chemistry, in: CRC Handbook of Chemistry and Physics, 97th ed., CRC Press, 2016, pp. 5–87, https://doi.org/10.1201/9781315380476.
- [28] J. Barbier, L. Oliviero, B. Renard, D. Duprez, Catalytic wet air oxidation of ammonia over M/CeO2 catalysts in the treatment of nitrogen-containing pollutants, Catal. Today 75 (1-4) (2002) 29–34, https://doi.org/10.1016/S0920-5861(02)00040-8.

- [29] G.S. Goff, G.T. Rochelle, Monoethanolamine degradation: O2 mass transfer effects under CO2 capture conditions, Ind. Eng. Chem. Res. 43 (20) (2004) 6400–6408, https://doi.org/10.1021/ie0400245.
- [30] L. Dumée, C. Scholes, G. Stevens, S. Kentish, Purification of aqueous amine solvents used in post combustion CO2 capture: a review, Int. J. Greenh. Gas. Control 10 (2012) 443–455, https://doi.org/10.1016/J.IJGGC.2012.07.005.
- [31] F. Jin, Y. Cui, Z. Rui, Y. Li, Effect of sequential desilication and dealumination on catalytic performance of ZSM-5 catalyst for pyridine and 3-picoline synthesis, J. Mater. Res 25 (2) (2010) 272–282, https://doi.org/10.1557/JMR.2010.0033.
- [32] A. Rey, et al., Amine degradation in CO2 capture. 2. new degradation products of MEA. Pyrazine and alkylpyrazines: analysis, mechanism of formation and toxicity, Int. J. Greenh. Gas. Control 19 (2013) 576–583, https://doi.org/10.1016/J. LIGGC.2013.10.018.
- [33] J.M. Colom-Díaz, M.U. Alzueta, Z. Zeng, M. Altarawneh, B.Z. Dlugogorski, Oxidation of H2S and CH3SH in a jet-stirred reactor: experiments and kinetic modeling, Fuel 283 (2021) 119258, https://doi.org/10.1016/j.fuel.2020.119258.
- [34] M.M. Dipippo, K. Sako, J.W. Tester, Ternary phase equilibria for the sodium chloride-sodium sulfate-water system at 200 and 250 bar up to 400°C, Fluid Phase Equilib. 157 (1999) 229–255, https://doi.org/10.1016/S0378-3812(99)00039-4.
- [35] R.V. Shende, V.V. Mahajani, Kinetics of wet oxidation of formic acid and acetic acid, Ind. Eng. Chem. Res. 36 (11) (1997) 4809–4814, https://doi.org/10.1021/ ie970048u.
- [36] J. Beyer, A. Goksøyr, D.Ø. Hjermann, J. Klungsøyr, Environmental effects of offshore produced water discharges: a review focused on the Norwegian continental shelf, Mar. Environ. Res. 162 (2020) 105155, https://doi.org/ 10.1016/j.marenvres.2020.105155.
- [37] A.F. Nielsen, A. Baun, S.I. Andersen, L.M. Skjolding, Critical review of the OSPAR risk-based approach for offshore-produced water discharges, Integr. Environ. Assess. Manag. 19 (5) (2023) 1172–1187, https://doi.org/10.1002/jeam.4715.
- [38] E. Saouter, D. Wolff, F. Biganzoli, D. Versteeg, Comparing options for deriving chemical ecotoxicity hazard values for the european union environmental footprint, part II, Integr. Environ. Assess. Manag. 15 (5) (2019) 796–807, https:// doi.org/10.1002/jeam.4169.